





Significant effort to develop alternative electrode materials, such as carbon aerogels (CAGs) and carbon nanotubes (CNTs) has had limited success. Electrodes based on CAGs requires no binder, yet the accessibility of micropores during activation remains questionable [13]. CNTs offer a unique combination of high porosity and low electrical resistivity. The CNT-based electrode research experienced rapid evolution from entangled multi-wall CNTs [14, 15] to open end, vertically aligned CNTs (VCNTs) [16]. Research on CNT based ultracapacitors is still undergoing, but the low volumetric density and difficulty in controlling the pore size limit their development and utilization.

The discovery of graphene - one-atom-thick planar sheet of  $sp^2$  bonded carbon atoms in a hexagonal lattice - has drawn tremendous attention due to its exotic material properties. Graphene has extraordinarily high material properties such as specific surface area ( $2,630 \text{ m}^2/\text{g}$ ) [17], charge carrier mobility ( $\sim 200,000 \text{ cm}^2/\text{Vs}$ ) [18], Young's modulus ( $1,100 \text{ GPa}$ ) [19], and thermal conductivity ( $\sim 5,000 \text{ W/mK}$ ) [20]. More importantly, in contrast to the conventional electrode materials, the effective surface area of the graphene does not depend on the distribution of pores due to its unique 2-D structure. Thus the utilization efficiency of surface can be significantly increased.

Some studies on graphene-based ultracapacitors have been reported [17, 21, 22]. Graphene was expected to have improved energy density by higher surface area, and reduced ESR by decreasing the ionic diffusion resistance. However, the energy/power values reported were much lower than the theoretical calculations. This could be the result of poor graphene quality or due to graphene in an agglomeration rather than extended morphology [17]. Obtaining controlled extended morphology is essential for maximum surface utilization.

There are several ways to create 2D graphene including peeling off thin layers from graphite plates by sticky tape and transferring platelets to substrates, epitaxial growth on SiC or metal (Ni, Cu etc) substrates, chemical reduction, and unzipping CNTs by plasma etching or chemical reactions. Chemical reduction because of its simplicity cost effectiveness, low temperature process, possible mass production, etc. has received a majority of the scientific interest as a method for graphene synthesis. Chemical reduction is based on a top down methodology, where the graphite is used as a precursor material. Graphite is exfoliated and oxidized into graphene oxide (GO) which is functionalized with oxygen containing functional groups such as hydroxyl, carboxyl and epoxide groups at the edge and/or on the 2D plane as shown in Figure 3 (a). For synthesis graphene, the GO should be reduced to functional group-free  $sp^2$ -hybridized graphene layers (Figure 3 (b)).

**Figure 3. Oxidized/functionalized graphene (GO) (a) and reduced graphene (b).**

A few approaches for the reduction have been proposed, including high temperature treatment (over  $1500^\circ\text{C}$ ) and chemical reduction with or without temperature assist. In this paper, we propose the use of microwave as an ultra fast heating source for reduction, under dry condition even without chemical assists. Previous studies on MW heating as a reduction source were reported where they used MW for heating dielectric media such as reducing agents [23] or polar solvents [24], rather than heating GO directly. Graphite [25] and carbon nanotubes (CNTs) [26] have been known as good microwave absorbers. We had reported the reduced CNT defects by MW annealing [27~30]. Graphene, a basic structural element of those carbon allotropes and its derivative GO are expected to have similar MW absorbing properties.

In this paper, a study on MW reduced graphene [31] is discussed and characterizations (Raman spectra, X-ray photoelectron spectroscopy (XPS), thermal/electrical properties and Raman spectra, X-ray photoelectron spectroscopy (XPS), thermal/electrical properties and electrochemical performance) of MW reduced graphene oxide is used to confirm graphene formation with the potential application as an electrode material in ultracapacitors.

## Experiments

Graphite flakes used were donated from Asbury Corp. All the chemicals were of analytical reagent grade, and used without further purification. GO was synthesized by Hummer's method [32]. Graphite was put into cold concentrated  $\text{H}_2\text{SO}_4$  and  $\text{NaNO}_3$  solutions in a flask. After graphite was mixed homogeneously,  $\text{KMnO}_4$  was slowly added to the flask and temperature was kept below  $20^\circ\text{C}$ . The mixture was stirred in an ice bath for 2 h and then in a  $35^\circ\text{C}$  water bath for 0.5 h.  $70^\circ\text{C}$  DI water was added into the flask drop by drop and the generated heat during adding water will keep the solution temperature around  $98^\circ\text{C}$ . The mixture was diluted by  $70^\circ\text{C}$  DI water and 30%  $\text{H}_2\text{O}_2$  until the reaction terminated. The mixture was filtrated and washed several times with DI water. The resulting GO solid was centrifuged for 30 min. The obtained supernatant was dried overnight to form GO films.

In a typical reduction experiment, the as-made dry GO was cut into a  $2 \text{ cm} \times 1 \text{ cm}$  size film and placed in a Pyrex

beaker. The film sample was then subjected to a microwave field (500 W,  $6.425\text{ GHz} \pm 1.285\text{ GHz}$ ) in a variable frequency microwave system (Microcure 2100). The surface temperature of the GO sample was monitored in real-time by an infrared thermometer.

When observing the evolution from GO to reduced GO in both the Microcure 2100 system and the household microwave oven, we added a quota of 2 mL 1mg/ml GO solution into a beaker and dried at  $55\text{ }^{\circ}\text{C}$ . Compared with the  $2\text{ cm} \times 1\text{ cm}$  size dry film, the smaller quantity of the starting GO absorbed less power and better contact with the beaker bottom increased the heat dissipation from GO to the substrate, then the reduction transition was slowed down enough to observe the whole process.

Scanning electron microscopy (SEM, JEOL 1530), atomic force microscopy (AFM, Veeco, operated at tapping mode), micro-Raman spectroscopy (Aramis, HORIBA Jobin Yvon) assembled with a confocal imaging microscope, X-ray photoelectron spectroscopy (XPS, SSX-100), and thermal gravity analysis (TGA) were used to characterize GO and the as-prepared reduced Graphene.

In order to prepare a thin film working electrode for electrochemical testing, 47.5 mg of graphene powder were dispersed in a glass vial containing an 1 ml *N*-Methyl-2-pyrrolidone (NMP) solution (containing 2.5 mg of Polyvinylidene Fluoride, PVDF) and ultra-sonicated for 30 min to obtain a uniform slurry. Then, 10  $\mu\text{L}$  of slurry was transferred onto a glassy carbon electrode embedded in a PTFE holder. The whole electrode was oven-dried in air for 30 min to evaporate NMP. The graphene loading was estimated to be 0.475 mg. The same procedure used for the preparation of the electrode based on the commercial activated carbon (Norit Supra 30, BET surface area;  $1,900\text{ m}^2/\text{g}$ ) for comparison.

In the characterization of electrochemical behavior, a glassy carbon disk (geometric area =  $0.196\text{ cm}^2$ ) and a platinum electrode were used as the working and the counter electrode, respectively. The Saturated Calomel Electrode (SCE) was used as the reference electrode and a  $1\text{ M H}_2\text{SO}_4$  solution was used as the electrolyte. Cyclic voltammetry (CV) was performed in a potential range from 0 to  $0.8\text{ V}$  (vs. SCE) at a potential scan rate of 10 to  $100\text{ mV/sec}$ . The galvanostatic charge-discharge experiments were performed at a constant current density of 0.1 to  $10\text{ mA/cm}^2$  to estimate the specific capacitance (F/g). For a benchmark electrode material, a commercial activated carbon (Norit Supra30, BET surface area;  $1,900\text{ m}^2/\text{g}$ ) was employed.

## Results and Discussions

### GO to Reduced GO

The GO reduction process mainly includes the removal of oxygen containing functional groups such as hydroxyl, carboxyl and epoxy groups on GO. When GO goes through the reduction process, its color dramatically changes. In dilute solutions, the color difference between graphene oxide and reduced graphene is prominent; as shown in Figure 4. The oxidized graphite exhibits brown color while the reduced GO appears very dark close to black. AFM height images indicated the thickness of the graphene oxide ranged from

0.36 nm to 1.69 nm, corresponding to 1~5 atomic graphene layers.

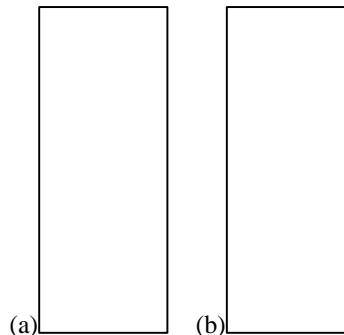


**Figure 4. Graphene oxide (a) and reduced GO (b) in a DMF/water mixture.**

We observed that microwave reduction induces local heating of GO and the decomposition rate of the functional groups such as epoxide and hydroxyls on GO may exceed the diffusion rate of the evolved gases such as  $\text{CO}_2$  or  $\text{CO}$ . This generates a high gas pressure in between GO layers exceeding Van der Waals force in-between layers, resulting in exfoliation of the graphene layers. This pressure makes a more granulated textures of the reduced GO compared to GO films, as shown in Figure 5.

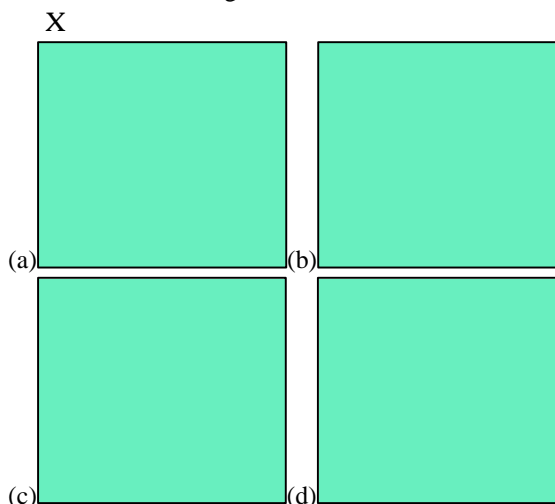


**Figure 5. SEM images of GO, top (a) and side views (b), of reduced GO, top (c) and side view (d).**

The reduced electrical resistance is another signature of GO conversion to reduced GO. The functionalized (oxidized) sites on the GO plane and along the edge break the structure regularity and are considered as structure defects, which hinder electron and phonon transport via x-y planes resulting in lowering electrical and thermal conductivity. The reduction process removes the defective functional groups, and improves the electronic and thermal transport properties. We observed the surface resistance of GO films in the range of  $1\sim 100\text{ M}/\text{sq}$  level. We found a dramatic decrease in resistance during all reduction methods including chemical, electric field and microwave assisted reductions. In particular,

the surface resistance of MW reduced GO decreased from  $10^4 \text{ M } \Omega/\text{sq}$  to around  $40 \text{ } \Omega/\text{sq}$ , yielding an electrical conductivity comparable with that of the exfoliated graphene at  $1050^\circ\text{C}$  [32], and about three orders of magnitude lower than chemically reduced GO by hydrazine [33], photo catalytic reduced GO [35] and GO after multi-step low-temperature annealing [35].

Raman G, D and 2D modes of graphene can determine linear defect density and electron-phonon coupling [2]. Raman spectra of a GO display two prominent G and D peaks at  $1583$  and  $1347 \text{ cm}^{-1}$ , respectively. In particular, the G band of GO is shifted to that of typical graphite [3]. This is mainly due to increased active defects [4], isolated double bonds of functional groups of GO [5] and a reduced number of stacked sheets [6,7,8]. The G peak is related to the vibration of  $\text{sp}^2$ -hybridized carbon and the D peak, corresponding to the conversion of an  $\text{sp}^2$ -hybridized carbon to a  $\text{sp}^3$ -hybridized carbon [37]. Figure 6 shows that the reduction makes the G band shifted down to  $1565 \text{ cm}^{-1}$ , indicating the recovery of the hexagonal network of carbon atoms [37]. Since the D/G ratio is inversely proportional to the average size of the  $\text{sp}^2$  domains and defects, the diminished D/G ratio in Figure 6 indicates that the MW reduction dramatically increased the average size of the crystalline graphene domains and removed defects such as functionalized sites.

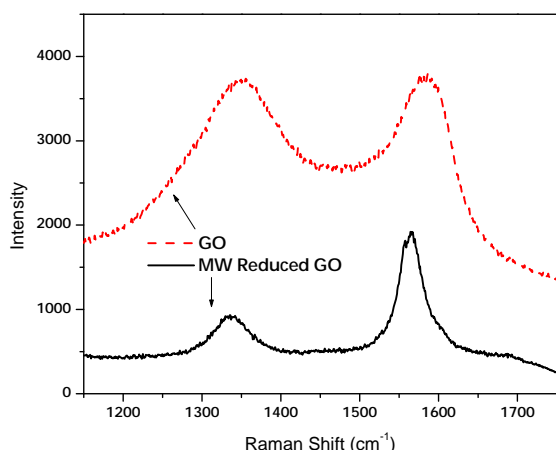


**Figure 6. Raman spectra of GO and reduced GO.**

The decomposition of carbonyl and hydroxyl groups on GO by MW reduction was confirmed by FTIR and XPS. The high-resolution C1s XPS spectra of the reduced graphene showed a significant decrease of oxygen-functionalized groups at  $286.1 \text{ eV}$  (C-OH),  $287.6 \text{ eV}$  (C=O), and  $289 \text{ eV}$  (O=C-OH) after MW reduction, confirming that most of the epoxide, hydroxyl and carboxyl groups were successfully removed.

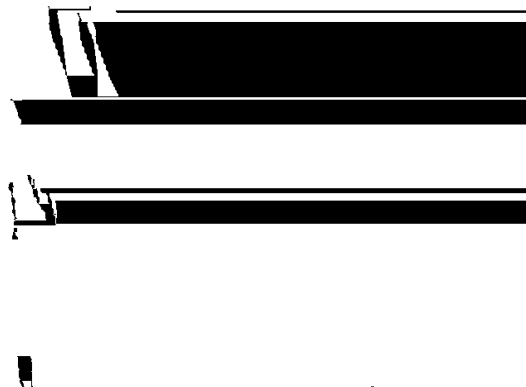


**Figure 7. Weight loss of GO and reduced GO in TGA.**

Figure 7 shows weight loss of GO and reduced GO in TGA. Significant weight loss from GO at  $\sim 180^\circ\text{C}$  was observed, which is believed to be corresponding to decomposition, degassing and evaporation of oxygen functional groups to  $\text{CO}_2$  or  $\text{CO}$ , and remaining chemical substances. Above  $200^\circ\text{C}$ , the weight loss continues. This loss may be from the loss of residual functional groups on the reduced GO. On the other hand, the reduced GO showed high thermal stability and weight loss starts over  $700^\circ\text{C}$ . Less defective carbons materials show high thermal stability, this phenomenon has been also demonstrated in carbon nanotubes (CNT) by our group [28, 29]. The TGA study on annealed CNTs showed that well-annealed CNTs have higher thermal decomposition temperatures, much higher elastic modulus and increased thermal transport capability, while overexposed CNTs showed poor properties. An optimized treatment condition needs to be used to maximized performance.

To compare capacitive behavior of the graphene with that of a commercial activated carbon, cyclic voltammetry curves and galvanostatic charge-discharge curves of both samples were recorded at room temperature in a  $1 \text{ M H}_2\text{SO}_4$  solution using a three-electrode configuration.

Shown in Figure 8 (a) are the typical cyclic voltammetry curves measured at a scan rate of  $10 \text{ mV/sec}$ . The amounts of the active materials (graphene and activated carbon,  $95 \text{ wt. \%}$  of total mass) were kept the same (ca.  $0.475 \text{ mg}$ ) for both samples and the current densities were normalized to the mass of the active materials. Clearly, the graphene-based electrode showed higher capacitance (larger current) than that of the activated carbon samples within the potential range of  $0.0\sim 0.8 \text{ V}$  (vs. SCE). The observed enhancement might be attributed to the unique structure of the graphene, which has a large surface area for facile charge-separation (electrochemical double-layer formation).

To calculate the specific capacitance ( $\text{F/g}$ ) of the graphene, charge-discharge curves were recorded at a constant current density of  $0.1$  to  $10 \text{ mA/cm}^2$ . Shown in Figure 8 (b) are the typical charge-discharge curves measured at a constant current density of  $2 \text{ mA/cm}^2$ . The specific capacitance of graphene was  $\sim 147.5 \text{ F/g}$  (as calculated from the discharge curve collected at  $10 \text{ mA/cm}^2$ ), which is  $\sim 1.6$  times that of the commercial activated carbon ( $87.8 \text{ F/g}$ ),

suggesting that the graphene has a great potential for ultracapacitor applications. Further investigations to elucidate the large capacitive behavior of graphene are still under way.

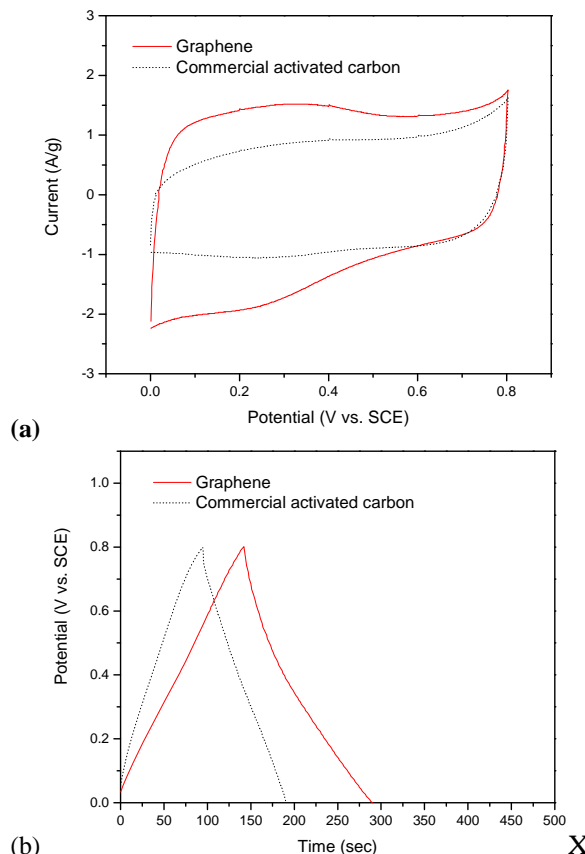


**Figure 8. Comparison of capacitive behavior of graphene and activated carbon in 1M H<sub>2</sub>SO<sub>4</sub> solution at room temperature. (a) Cyclic voltammetry curve measured with a voltage scan rate of 10 mV/sec. (b) Galvanostatic charge-discharge curve at a current density of 2 mA/cm<sup>2</sup>.**

## Conclusions

Graphene, the basic building block of graphitic materials was successfully synthesized from the microwave-assisted reduction, which includes creating GO from graphite particles and reducing back to graphene.

Various characterizations such as color, electric resistance, Raman spectra, XPS, AFM and TGA confirmed the new MW reduction as a fast effective method for generating high quality graphene from GO.

The ultracapacitor electrode performance of the reduced GO was investigated. The preliminary electrochemical test showed that the MW reduced GO exhibited almost two times higher specific capacitance than that of activated carbon used, the state of the art electrode material in commercial ultracapacitors. This might be because graphene synthesized is of considerably high quality and its high surface area was of high quality. Great potential of the reduced GO for a next generation electrode material in high-energy storage devices was demonstrated. Further studies on device level testing, graphene layers' gap control and etc. are on going.

## Acknowledgments

Authors would like to thank National Science Foundation (NSF, CMMI#0800849) for financial support, and Drs. Linda Zhong with Maxwell Technologies, Inc., and Michael Hu with Oak Ridge National Lab for valuable discussions.

## References

1. Beker H, et. al., "Low voltage electrolytic capacitor", *US patent*, US2800616, 1957.
2. Geim A, and Novoselov K, "The rise of graphene", *Nature Materials*, Vol. 6, No. 3, (2007), pp. 183–191.
3. Pimenta M, Dresselhaus G and et al., "Studying disorder in graphite-based systems by Raman spectroscopy", *Phys. Chem. C*, Vol. 9, (2007) pp. 1276-1291.
4. Ganganahalli K. Ramesha and Srinivasan S, "Electrochemical Reduction of Oriented Graphene Oxide Films: An in Situ Raman Spectroelectrochemical Study", *Phys. Chem. C*, vol. 113, No. 19, (2009), pp 7985–7989.
5. Cancado, L. G.; Pimenta, M. A.; Neves, B. R. A.; Dantas, M. S. S.; Jorio, "Influence of the Atomic Structure on the Raman Spectra of Graphite Edges", *A. Phys. Rev. Lett.*, Vol. 93, (2004), pp. 247401.
6. Ferrari, A. C.; Robertson, "Interpretation of Raman spectra of disordered and amorphous carbon", *J. Phys. Rev. B*, Vol. 61, (2000), pp. 14095.
7. Ferrari, A. C.; Meyer, J. C.; Scardaci, V.; Casiraghi, C.; Lazzeri, M.; Mauri, F.; Piscanec, S.; Jiang, D.; Novoselov, K. S.; Roth, S.; Geim, A. K., "Raman Spectrum of Graphene and Graphene Layers", *Phys. Rev. Lett.* Vol. 97, (2006), pp. 187401.
8. Gupta, A.; Chen, G.; Joshi, P.; Tadigadapa, S.; Eklund, P. C. "Raman Scattering from High-Frequency Phonons in Supported n-Graphene Layer Films", *Nano Lett.* Vol 6, (2006), pp. 2667.
9. Graf, D.; Molitor, F.; Ensslin, K.; Stampfer, C.; Jungen, A.; Hierold, C.; Wirtz, L. "Spatially Resolved Raman Spectroscopy of Single- and Few-Layer Graphene", *Nano Lett.* Vol. 7, (2007), pp. 238.
10. Barisci, J.N., G.G. Wallace, D.R. MacFarlane, and R.H. Baughman, "Investigation of ionic liquids as electrolytes for carbon nanotube electrodes". *Electrochemistry Communications*, Vol. 6, No. 1, (2004), pp. 22-27.
11. Rudge, A., J. Davey, I. Raistrick, S. Gottesfeld, and J.P. Ferraris, "Conducting Polymers as Active Materials in Electrochemical Capacitors". *Journal of Power Sources*, Vol. 47, (1994), pp. 89-107.
12. Izmailova, M.Y., A.Y. Rychagov, K.K. Den'shchikov, Y.M. Vol'fkovich, E.I. Lozinskaya, and A.S. Shaplov, "Electrochemical Supercapacitor with Electrolyte Based on an Ionic Liquid". *Russian Journal of Electrochemistry*, Vol. 45, No. 8, (2009), pp. 949-950.
13. Zhang, L.L. and X.S. Zhao, "Carbon-based materials as supercapacitor electrodes", *Chemical Society Reviews*, Vol. 38, No. 9, (2009), pp. 2520-2531.
14. Kim, J.H., K.W. Nam, S.B. Ma, and K.B. Kim, "Fabrication and electrochemical properties of carbon nanotube film electrodes". *Carbon*, Vol. 44, No.10, (2006), pp. 1963-1968.

15. Kaempgen, M., J. Ma, G. Gruner, G. Wee, and S.G. Mhaisalkar, "Bifunctional carbon nanotube networks for supercapacitors", *Applied Physics Letters*, Vol. 90, No. 26 (2007), pp. 264104-2.
16. Lu, W., L. Qu, K. Henry, and L. Dai, "High performance electrochemical capacitors from aligned carbon nanotube electrodes and ionic liquid electrolytes", *Journal of Power Sources*, Vol. 189, No. 2, (2009), pp. 1270-1277.
17. Stoller, M.D., S. Park, Y. Zhu, J. An, and R.S. Ruoff, "Graphene-Based Ultracapacitors" *Nano Letters*, Vol. 8, No. 10, (2008), pp. 3498-3502.
18. Bolotin, K.I., K.J. Sikes, Z. Jiang, M. Klima, G. Fudenberg, J. Hone, P. Kim, and H.L. Stormer, "Ultrahigh electron mobility in suspended graphene", *Solid State Communications*, Vol. 146, No. 9, (2008), pp. 351-355.
19. Lee, C., X.D. Wei, J.W. Kysar, and J. Hone, "Measurement of the elastic properties and intrinsic strength of monolayer graphene", *Science*, Vol. 321, No. 5887, (2008), pp. 385-388.
20. Balandin, A.A., S. Ghosh, W.Z. Bao, I. Calizo, D. Teweldebrhan, F. Miao, and C.N. Lau, "Superior thermal conductivity of single-layer graphene", *Nano Letters*, Vol. 8, No. 3, (2008), pp. 902-907.
21. Wang, Y., Z.Q. Shi, Y. Huang, Y.F. Ma, C.Y. Wang, M.M. Chen, and Y.S. Chen, "Supercapacitor Devices Based on Graphene Materials", *Journal of Physical Chemistry C*, Vol. 113, No. 30, (2009), pp. 13103-13107.
22. Vivekchand, S.R.C., C.S. Rout, K.S. Subrahmanyam, A. Govindaraj, and C.N.R. Rao, "Graphene-based electrochemical supercapacitors", *Journal of Chemical Sciences*, Vol. 120, No. 1, (2008), pp. 9-13.
23. Hassan, H. M. A.; Abdelsayed, V.; Khder, A. E. R. S.; AbouZeid, K. M.; Ternier, J.; El-Shall, M. S.; Al-Resayes, S. I.; El-Azhary, A. A. "Microwave synthesis of graphene sheets supporting metal nanocrystals in aqueous and organic media", *J. Mater. Chem.* Vol. 19, (2009), pp. 3832-3837.
24. Murugan, A. V.; Muraliganth, T.; Manthiram, A. "Rapid, Facile Microwave-Solvothermal Synthesis of Graphene Nanosheets and Their Polyaniline Nanocomposites for Energy Storage", *Chem. Mater.* Vol. 21, (2009), pp. 5004-5006.
25. Fan, Y, Yang, H, Li, M, Zou, G., "Evaluation of the Microwave Absorption Property of Flake Graphite", *Mater. Chem. Phys.* Vol. 115, (2009), pp. 696-698.
26. Wu, J.; Kong, L., "High microwave permittivity of carbon nanotube composites", *Appl. Phys. Lett.* Vol. 84, (2004), pp. 4956-4958.
27. Sunden E, Moon K, Wong C. , King W. and Grahama S, "Microwave assisted patterning of vertically aligned carbon nanotubes onto polymer substrates", *J. Vac. Sci. Technol. B*, Vol. 24, No. 4, (2006), pp. 1947.
28. Moon K, Lin W, Jiang H, Ko H, Zhu L, and Wong C, "Surface treatment of MWCNT array and its polymer composites for TIM application" *58th Electro. Comp. Technol. Conf.*, 27-30 May 2008 pp. 234 – 237.
29. Lin, W., Moon K, Zhang S, Ding Y, Shang J, Chen M, and Wong C, "Microwave Makes Carbon Nanotubes less Defective", *Acs Nano*, February 17, 2010 in Article ASAP, **In press**.
30. Lin, W., Moon K, and Wong C, A "Combined Process of In Situ Functionalization and Microwave Treatment to Achieve Ultrasmall Thermal Expansion of Aligned Carbon Nanotube-Polymer Nanocomposites: Toward Applications as Thermal Interface Materials", *Advanced Materials*, Vol. 21, No. 23, (2009), pp. 2421-2424.
31. Li, Z., Yao Y, Lin Z, Moon K, Lin W, and Wong C, "Ultrafast, Dry Microwave Synthesis of Graphene Sheets", *Journal of Materials Chemistry*, 2010. **In review**.
32. William S. Hummers Jr., and Richard E. Offeman "Preparation of Graphitic Oxide", *J. American Chemical Society*, Vol. 80, No. 6, (1958), pp. 1339–1339.
33. Schniepp, H. C.; Li, J.-L.; McAllister, M. J.; Sai, H.; Herrera-Alonso, M.; Adamson, D. H.; Prud'homme, R. K.; Car, R.; Saville, D. A.; Aksay, I. A., "Functionalized Single Graphene Sheets Derived from Splitting Graphite Oxide", *J. Phys. Chem. B* Vol. 110, (2006), pp. 8535-8539.
34. Stankovich, S.; Dikin, D. A.; Piner, R. D.; Kohlhaas, K. A.; Kleinhammes, A.; Jia, Y.; Wu, Y.; Nguyen, S. T.; Ruoff, R. S. "Synthesis of graphene-based nanosheets via chemical reduction of exfoliated graphite oxide", *Carbon*, Vol. 45, (2007), pp. 1558-1565.
35. Williams, G.; Seger, B.; Kamat, P. V., "TiO<sub>2</sub>-Graphene Nanocomposites. UV-Assisted Photocatalytic Reduction of Graphene Oxide", *Acs Nano*, Vol. 2, (2008), pp. 1487-1491.
36. Lu, G.; Ocola, L. E.; Chen, "Reduced graphene oxide for room-temperature gas sensors", *J. Nanotechnol.* Vol. 20, (2009), pp. 445502.
37. Kang, H.; Kulkarni, A.; Stankovich, S.; Ruoff, R. S.; Baik, S., "Restoring electrical conductivity of dielectrophoretically assembled graphite oxide sheets by thermal and chemical reduction techniques", *Carbon* Vol. 47, (2009), pp. 1520-1525.
38. Ramesha, G. K.; Sampath, S. "Electrochemical Reduction of Oriented Graphene Oxide Films: An in Situ Raman Spectroelectrochemical Study", *J. Phys. Chem. C*, Vol. 113, (2009), pp. 7985-7989.